Robustified Distributed Model Predictive Control for Coherence and Energy Efficiency-Aware Platooning

Conference Paper · July 2019

DOI: 10.23919/ACC.2019.8814866

CITATIONS
10

READS
199

2 authors:

Massimo Zambelli
University of Pavia
14 PUBLICATIONS **115** CITATIONS

SEE PROFILE

Antonella Ferrara
University of Pavia
475 PUBLICATIONS **12,031** CITATIONS

SEE PROFILE

Robustified Distributed Model Predictive Control for Coherence and Energy Efficiency-Aware Platooning

Massimo Zambelli and Antonella Ferrara*

***Abstract*— Platooning has become one of the most appealing formations for intelligent vehicles safety enhancement and traffic regulation. Besides the traditional control algorithms, which are required to enforce at least local and string stability, more complex control schemes can be designed to cope with advanced requirements. In this paper, a suitable Distributed Model Predictive Control (DMPC) scheme, robustified with a second-order Integral Sliding Mode (ISM) correction term, is proposed to enforce and maintain coherence during cruising, while considering energy efficiency during acceleration/deceleration phases. While the former aspect has a complex impact on traffic regulation, especially when a large number of vehicles is considered, the latter is of primary importance in an increasingly eco-friendly transportation systems design. The proposed approach is well suited for real-world implementation, and can constitute a valid basis for more advanced control architectures. Simulation results highlight the effectiveness of the proposed architecture in maintaining the formation while guaranteeing a robust achievement of the required performance.**

I. INTRODUCTION

In the last decades the increase in complexity and availability of intelligent vehicles has moved the research focus onto advanced formation control problems. Among many possibilities, platooning (schematized in Figure 1) has attracted a lot of interest for its simplicity and effectiveness in improving safety, comfort and fuel consumption, while allowing for improvements in traffic regulation [1]. Many studies have been carried out from both control and network architecture perspectives (see, e.g., [2], [3] and references therein), in order to improve the effectiveness and realizability of the proposals in a real-world scenario. In particular, robustness remains one of the major issues [4]. Two fundamental requirements, namely local and string stability, are crucial in a platoon control system and must be guaranteed despite uncertainties which, in practice, always affect the considered dynamics. Basing on (distributed) optimal control concepts, additional requirements can be addressed, with the aim of further enhancing the effectiveness of the platoon formations [5]–[7]. Energy efficiency appears to be a natural objective in an evolved formation management system [8], due to the obvious environmental and economic benefits that follow. While electric (EVs) and hybrid (HEVs) vehicles have become a valuable resource in lowering the pollution emissions and increasing efficiency via regenerative braking systems, a more intelligent management of the energy stored in the vehicle battery packs can be achieved through predictive control during acceleration and deceleration maneuvers.

*Dipartimento di Ingegneria Industriale e dell'Informazione, University of Pavia, via Ferrata 5, 27100 Pavia, Italy massimo.zambelli01@universitadipavia.it, a.ferrara@unipv.it

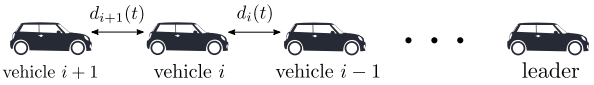

Fig. 1. Basic idea of a platoon.

During cruising, when vehicles proceed instead at constant relative distance, e.g. on highways, coherence becomes a valuable feature. It can be informally defined as the ability of the formation to behave like a rigid body, which implies that the distance between the two extremal vehicles (the leader and the last follower) remains constant and equal to a prespecified one [9]. It is especially important in a context characterized by traffic regulation, in particular if a large number of vehicles is considered [10]. Despite the enforcement of local and string stability, as highlighted for instance in [11], coherence cannot be in principle guaranteed in the presence of unknown perturbations of the acceleration, which in a practical framework can be due to uncertainties in the vehicle dynamics modelling and evolution.

In this paper, a non-iterative non-cooperative Distributed Model Predictive Control (DMPC) scheme is proposed for the control of an arbitrary number of vehicles in platoon configuration. Besides safety, coherence is regarded as the primary objective, while energy efficiency is pursued as a valuable feature. In contrast with the works already present in the literature, which usually achieve robustness through complex control schemes, the present work proposes the introduction of an additional second-order Integral Sliding Mode (ISM) controller [12], which works at a higher rate than the MPC, with the aim of compensating matched disturbances. The resulting system is enabled to follow the nominal predicted behaviour during each control step. As a matter of fact, it can be evidenced that the closed-loop control scheme becomes far less sensitive to the MPC sampling time, so that lower optimization frequencies can be employed without affecting the quality of the results. This, in turn, enables for less computational power and packet transmission rates requirements, with obvious benefits both from a local and a networked standpoint.

In order to allow the description of a more general situation in which, for instance, an higher-level controller is employed to that end (e.g. a traffic regulation system, which controls the steady-state platoon speed [13]), the leader is kept uncontrolled. EVs are considered in the discussion, so that also an electric model is proposed in order to take into account regenerative braking. In different cases, such description can simply be neglected. The resulting platoon regulation system is well suited for practical implementation due to the very limited resources requirements (a noticeable property is

This is the final version of the paper, accepted for publication in the Proceedings of the 2019 American Control Conference, Philadelphia, July 2019.

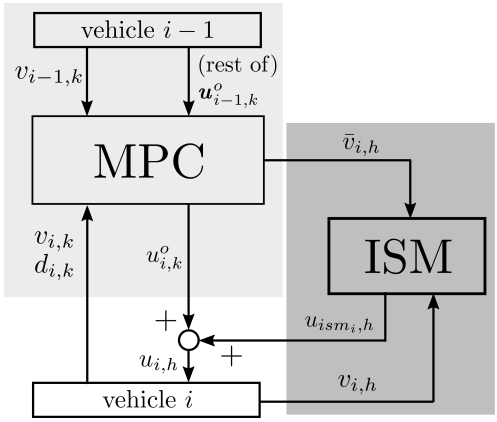

Fig. 2. Schematic of the multirate control system. The brighter gray box indicates a slower rate (sampling time T_s), while the darker box refers to the higher one (sampling time t_s).

that global position information is not required). Simplicity and flexibility make the proposed approach a good basis on which more complex control architectures could be designed.

It is worth noticing that sliding mode control has already been successfully utilized in vehicle control (see [14]) and, in particular, in vehicle platooning [15], [16].

The paper is organized as follows. In Section II the vehicles model is described, both from a kinematic (Subsection II-A) and electric (II-B) point of view. The main results of this work are then presented in Section III, where the MPC problem is formulated (III-A) and the ISM robustification scheme is presented (III-B). Simulation results, in Section IV, highlight the effectiveness of the proposed approach and, finally, section V concludes the paper.

II. VEHICLES MODEL

In this section a kinematic description of the single vehicles involved in the platoon is proposed. The differences between such a model and the real vehicle dynamics are explicitly described by means of uncertainty terms, in order to formally prove the robustness of the proposed control approach in the following. An electric power flow representation is also introduced for the case in which vehicles are EVs or HEVs able to exploit regenerative braking.

A. Kinematic Model

The (one-dimensional) absolute position $p(t)$ along the platoon path and velocity $v(t)$ of each vehicle can be modelled as

$$\begin{cases} \dot{p}(t) = v(t) \\ m\dot{v}(t) = F_{in}(t) - F_{loss}(v(t)) + \delta(t) \end{cases} \tag{1}$$

where m is the vehicle mass, while $F_{loss}(v(t))$ encompasses the aerodynamic drag and rolling resistance forces such that

$$F_{loss}(v(t)) = \frac{1}{2}\rho C_a S v^2(t) + C_r m g v(t) \tag{2}$$

with ρ the air density, C_a the aerodynamic coefficient, S the equivalent vehicle surface, C_r the rolling resistance coefficient and g the gravitational acceleration. The term $\delta(t)$ is the uncertainty in the description of a real vehicle plant by means of model (1), and includes for instance parameters mismatch and unaccounted time-varying effects. As an example, aerodynamic and rolling resistance coefficients are often nominal values obtained via experiments in specific conditions, and the vehicle mass can change due to the presence of a different number of passengers.

As for the input force $F_{in}(t)$, let us introduce the following

Assumption 1: The vehicle is equipped with a low-level fast enough slip controller, able to maintain the desired slip ratio while keeping the tire-road friction characteristic in the linear region (see e.g. [17]). Then, being $\omega_l(t)$ the l-th wheel rotational speed, one has

$$\dot{\omega}_l(t) \simeq 0 \quad \forall t \tag{3}$$

i.e. a steady state condition is considered, so that at each time instant the forces exerted at the wheels level can be considered as coincident with that in output from the powertrain. Therefore,

$$\sum_{l \in DW} \frac{T_{in_l}(t)}{R_{e_l}} = F_{in}(t) \tag{4}$$

where DW is the set of driving wheels, T_{in_l} is the net torque applied to the l-th wheel (supposed equal for the two wheels on the same axle) and R_{e_l} its effective radius.

From Assumption 1, two consequences can be drawn:

- The scope of validity of model (1) coincides with a limited range of input forces $F_{in}(t)$, corresponding to the linear region of the tire-road friction characteristic curve. This implies a non-negligible saturation in the range

  $$F_{in}(t) \in [F_{min}(t); F_{max}(t)] \tag{5}$$

  with bounds dependent on the specific properties of the tires and the condition of the road.
- Having neglected the major effects of a transient in the generation of the tire-road forces, it appears reasonable to assume that the actually exerted force $F_{in}(t)$ follows a first-order dynamics with respect to the one requested, namely

  $$\tau \dot{F}_{in}(t) = F_e(t) + F_b(t) - F_{in}(t) + \gamma(t) \tag{6}$$

  where τ is the (possibly unknown) time constant, $F_e(t)$ is the *requested* electric force, which can be positive (during acceleration) or negative (during regenerative braking) and $F_b(t)$ is the *requested* mechanical braking force, obviously only negative. The term $\gamma(t)$, analogously to $\delta(t)$ in (1), describes the uncertainty in the representation of the real behaviour of $F_{in}(t)$ by means of (6).

Remark 1: Note that possible residual mismatch due to nominal effective radius imprecision and real slip control actuation, neglected by virtue of Assumption 1, can be suitably lumped into the matched uncertainty terms $\delta(t)$ and $\gamma(t)$ as well.

Remark 2: Although the distance between the vehicles has an obvious impact on the aerodynamic drag, in this work such an effect is neglected. Being cars, and not trucks, the main object of interest, only little savings can be achieved

in maintaining a tight formation. Moreover, since for safety reasons a Constant Time Headway (CTH) spacing policy is established, at high velocities (when such a gain would be significant) the vehicles are too far apart to actually experiment drag reduction.

B. Electric Model

An electric model of the powertrain is also required in order to optimize energy consumption and recovery through regenerative braking (see, e.g., [18]). The power flow is described here, so that during an MPC optimization horizon a net energy cost/gain will be in fact obtained. The total power utilized by the motors is

$$P_m(t) = \sum_{\mu \in M} T_{in_\mu}(t)\omega_\mu(t)\eta_\mu(T_{in_\mu}(t),\omega_\mu(t))^{-sign(T_{in_\mu}(t))} \tag{7}$$

where M is the set of electrical motors driving the vehicle wheels. The efficiency function $\eta_\mu(T_{in_\mu}(t),\omega_\mu(t))$ is specific of the particular motor μ, and is usually obtained via experiments (for a rough approximation, it could usually be assumed constant in the working region). The wheels rotational speeds in (7) can be approximated as

$$\omega_l(t) = \frac{g_{r_l}}{R_{e_l}} v(t) \tag{8}$$

where the gear ratio g_{r_l} is supposed here constant for the sake of simplicity, since the description is mainly referred to EVs. Nevertheless, a variable ratio can be considered for different vehicle configurations, with a possible additional degree of freedom in the control. Please note that the $sign(.)$ function at the exponent in expression (7) allows to describe also regenerative braking, in which the power flows "backwards", from the wheels to the engine. The total power entering (or exiting) the battery pack is then

$$P_b(t) = P_m(t)\eta_b^{-sign(F_{in}(t))} \tag{9}$$

with η_b the efficiency of the conversion from mechanical to chemical energy, supposed here constant for simplicity.

III. CONTROL ALGORITHM

In the proposed approach, each of the vehicles in the platoon is supposed to embed an independent controller and a short-distance Vehicle-to-Vehicle (V2V) communication device. The instantaneous velocity measurement is required, as well as the distance from the preceding vehicle (e.g. via a range sensor in the front bumper). Since the communication frequency is assumed comparable with that of control optimizations, the resulting architecture is designed basing on a distributed non-iterative MPC scheme. Considered a platoon composed of n vehicles, let us map them on indices such that 1 is associated to the leader, while the following vehicles are indexed in ascending order, for $i = 2,\cdots,n$. After the connection of a new vehicle i to the network, the preceding one, $i-1$, sends to it its nominal physical parameters. Then, at each iteration, the latter sends the computed optimal control sequence (except for the first element) to vehicle i, which at the successive iteration computes an updated prediction of the future distances from its predecessor. On the contrary, the local ISM correction term, as will be thoroughly explained in the following, is computed independently for each of the vehicles, with no interaction required among the neighbours. If all of the vehicles are equipped with the same proposed controller, this is sufficient to guarantee an ideal control of the entire formation, as shown both in theory and in simulation in the following.

A. Distributed MPC

For the i-th vehicle on-board controller, the following *nominal* model (not comprising uncertainty) is considered basing on (1)

$$\begin{cases} \dot{\bar{d}}_i(t) = \bar{v}_{i-1}(t) - \bar{v}_i(t) \\ \dot{\bar{v}}_{i-1}(t) = \frac{1}{m_{i-1}}\left(\bar{F}_{in_{i-1}}(t) - F_{loss_{i-1}}(\bar{v}_{i-1}(t))\right) \\ \dot{\bar{v}}_i(t) = \frac{1}{m_i}\left(\bar{F}_{in_i}(t) - F_{loss_i}(\bar{v}_i(t))\right) = \bar{f}_v(v_i(t),u_i(t)) \end{cases} \tag{10}$$

The term $\bar{d}_i(t)$ is the relative distance, which corresponds to

$$\bar{d}_i(t) = \bar{p}_{i-1}(t) - \bar{p}_i(t) \tag{11}$$

and is available for measurement (supposedly with ideal precision) through the range sensors mounted at the front of the i-th vehicle. The velocity $v_i(t)$ can be measured by assumption, and hence $v_{i-1}(t)$ can be made available by vehicle $i-1$ through short-range communication. Notice that the second equation in (10) is based on the nominal parameters received by i from $i-1$ at connection time.

For a generic $r = \{i-1, i\}$, the control input signal is

$$u_r(t) = u_{1_r}(t) + u_{2_r}(t) = F_{e_r}(t) + F_{b_r}(t) \tag{12}$$

As for the latter, two cases can be identified in practice with reference to Equation (6), which give rise to different control schemes.

Case 1: The actuators dynamics can be neglected, i.e.

$$\tau_r = 0 \;\Rightarrow\; \bar{F}_{in_r}(t) = u_r(t) \tag{13}$$

so that the final model is of order two as per (10).

Case 2: The actuators dynamics cannot be neglected, i.e.

$$\tau_r \neq 0 \;\Rightarrow\; \dot{\bar{F}}_{in_r}(t) = \frac{1}{\tau_r}\left(u_r(t) - \bar{F}_{in_r}(t)\right) \tag{14}$$

so that additional dynamics must be added to (10), and the final model becomes of order three. Notice that in this case, in the case of a state-feedback MPC formulation, also $\bar{F}_{in_r}$ must be available.

At each discrete time instant k, sampled with period T_s corresponding to the selected MPC routine time step, vehicle i computes an optimal control sequence $\boldsymbol{u}^o_{i,k} = \{u^o_{i,k}, \cdots, u^o_{i,(k+N)}\}$, $u^o_{i,k} = [u^o_{1_i,k}, u^o_{2_i,k}]^T$ solving a constrained optimization problem minimizing a cost function

$J_{i,k}$ over the N future steps (i.e. the prediction horizon). Then, following the receding horizon approach, only the first computed input $u^o_{i,k}$ is applied for the entire subsequent interval T_s. The rest of the control sequence is sent to vehicle $i+1$, which in the successive optimization, at time instant $k+1$, predicts $\bar{\boldsymbol{v}}_{i,(k+1)} = \{\bar{v}_{i,(k+1)}, \cdots, \bar{v}_{i,(k+1+N)}\}$ and $\bar{\boldsymbol{d}}_{i,(k+1)} = \{\bar{d}_{i,(k+1)}, \cdots, \bar{d}_{i,(k+1+N)}\}$ applying the received sequence to the stored nominal model of vehicle i (the last term is duplicated, in order to match the required length).

Remark 3: Even if the leader is considered independently controlled as a generalization, it is nevertheless required that it sends to the following vehicle the future $N-1$ control inputs, sampled at an according rate so that its nominal evolution can be computed by vehicle 2.

A CTH policy is used in this work, which has been proven to be suitable for locally communicating vehicles [19]. Such an approach aims at keeping constant the time t_{CTH} required by a vehicle to cover the distance from the preceding one. In formulae, the required distance $d_i(t)$ at any time instant is

$$d_i^{CTH}(t) = d_{min} + t_{CTH} v_i(t) \tag{15}$$

where d_{min} is a designed minimum distance, kept for safety when the vehicles are still.

In the algorithm proposed in the present paper, the i-th vehicle should minimize the following cost

$$J_{i,k} = \alpha_d c_{d,k} + \alpha_e c_{e,k} + \alpha_b c_{b,k} \tag{16}$$

where

$$c_{d,k} = \sum_{j=k+1}^{k+N} (\bar{d}_{i,j} - \bar{d}_{i,j}^{CTH})^2 \tag{17}$$

is the cost associated with the distances sequence predicted by means of (10),

$$c_{e,k} = \sum_{j=k+1}^{k+N} P_{m_i,j} \tag{18}$$

is the net energy outcome from usage and regeneration during the prediction horizon and

$$c_{b,k} = \sum_{j=k+1}^{k+N} F_{b_i,j}^2 = \sum_{j=k+1}^{k+N} u_{2_i,j}^2 \tag{19}$$

is the cost associated with the mechanical braking force. As a general rule, α_b should always be kept so large that the use of mechanical brake is discouraged unless inevitable. In fact, as already pointed out, regenerative braking is to be privileged in view of a reduction of wasted energy.

As for the constraints, the following appear fundamental for the practical effectiveness of the proposed algorithm

$$F_{min_i,k} + \kappa \le u_{1_i,k} + u_{2_i,k} \le F_{max_i,k} - \kappa \tag{20a}$$

$$0 \le \bar{v}_{i,k} \le v_{max,k} \tag{20b}$$

$$d_{min} \le \bar{d}_{i,k} \le d_{max,k} \tag{20c}$$

where κ will be introduced in the following. In particular, (20a) accounts for the saturations (5) given by the physical tire-road friction possibilities, the maximum torque exertable by the electric motors and the limit braking force. For safety and road speed limit purposes, (20b) and (20c) are also enforced with v_{max} and d_{max} possibly varying parameters.

B. ISM robustification

Given that the optimal control input $\boldsymbol{u}^o_{i,k}$ computed by the i-th vehicle at the time instant k is obtained relying on imprecise (nominal) models, optimality and even convergence cannot in principle be guaranteed for the real plant. In order to overcome this issue, the fundamental idea is that of having a trivial controller able to run at a higher rate which, in practice, compensates for the matched uncertainty so that the real system behaves as the nominal one. In this paper, a second-order Sub-Optimal Sliding Mode [20] is enforced, so that the resulting law is sufficiently smooth when it directly affects the acceleration (*Case 1*) but also suitable for *Case 2*, when the relative degree of the system is 2. In a practical implementation, the action of the ISM correction must of course be exerted at discrete time instants. In particular, having defined t_s as the ISM sampling time, the computation of the corrective control term is performed at discrete steps h of length t_s. At the same time instants velocity measurements are to be acquired and the total control $u_{i,h}$ is to be applied and held for the successive t_s seconds. A schematic of the complete resulting multirate scheme is reported for convenience in Figure 2.

For each vehicle i, let us now introduce the following

Assumption 2: With Δ_i, $\hat{\Delta}_i$ and Γ_i being known positive constants,

$$|\delta_i(t)| \le \Delta_i,\ |\dot{\delta}_i(t)| \le \hat{\Delta}_i,\ |\gamma_i(t)| \le \Gamma_i(t) \quad \forall t \tag{21}$$

The following so-called *sliding variable* can then be defined as

$$\sigma_{i,h} = v_{i,h} - \bar{v}_{i,h} \tag{22}$$

where $\bar{v}_{i,h}$ is the nominal velocity of vehicle i, computed relying on model (10) starting from the most recent previous MPC sampling time instant, i.e.

$$\bar{v}_{i,h} = v_i(kT_s) + \int_{kT_s}^{kTs+ht_s} \bar{f}_v(\bar{v}_i(t), u^o_{i,k})\ dt \tag{23}$$

Then, for the two considered cases, the total control input to be used in the h-th time step is

$$u_{i,h} = (u^o_{1_i,k} + u_{ism_i,h}) + u^o_{2_i,k} = \bar{u}_{i,h} + u_{ism_i,h} \tag{24}$$

while (10) is left evolving under the nominal

$$\bar{u}_{i,h} = u^o_{1_i,k} + u^o_{2_i,k},\ \ \forall h : kT_s \le ht_s < (k+1)T_s \tag{25}$$

The next propositions, stated for simplicity in continuous time hold, respectively, for the two considered cases.

Proposition 1: In *Case 1*, for the generic vehicle i and for a proper choice of K_i, if the corrective term is selected as

$$u_{ism_i,h} = u_{ism_i}(kT_s) - \int_{kT_s}^{kTs+ht_s} K_i sign\left(\sigma_i(t) - \frac{\sigma_i^*}{2}\right)\ dt \tag{26}$$

TABLE I

NOMINAL VEHICLES PARAMETERS

m [Kg]	$C_a \times S$ [m^2]	C_r	g_r	ρ [kg/m^3]
1200	0.8	0.008	10	1.22
η_m	η_t	η_b	τ	$\eta_\mu \ \forall \mu$
0.75	0.85	0.95	0.05	$\eta_m \eta_t$

TABLE II

SIMULATION PARAMETERS

N	T_s [s]	t_s	t_{CTH} [s]	K [N]
10	2	0.01	3	350
F_{min} [N]	F_{max} [N]	d_{min} [m]	d_{max} [m]	v_{max} [m/s]
-6500	6500	4	100	50

where σ_i^* is the value of $\sigma_i(t)$ at the last time instant when $\dot{\sigma}_i(t)=0$, the real velocity evolution tracks in finite time the nominal one, predicted relying on model (10).

Proof: The formal proof of the finite-time convergence for the Sub-Optimal Sliding Mode Control algorithm is given in [20]. Therefore, it suffices to verify that in the present case the needed hypothesis hold. Let us derive the expression of the derivatives of $\sigma_i(t)$, namely

$$\begin{aligned}\dot{\sigma}_i(t) &= \dot{v}_i(t) - \dot{\bar{v}}_i(t) \\ &= \frac{1}{m_i}(u_{ism_i}(t) - F_i^*(t) + \delta(t))\end{aligned} \tag{27}$$

with $F_i^*(t) = F_{loss_i}(v_i(t)) - F_{loss_i}(\bar{v}_i(t))$ a time-dependent component, locally bounded by $\bar{F}_i^* \geq 0$ and with first time-derivative locally bounded by $\hat{F}_i^* \geq 0$, since in practice velocities and accelerations can only assume values in a closed set. Therefore,

$$\ddot{\sigma}_i(t) = \frac{1}{m_i}\dot{u}_{ism_i}(t) + \frac{1}{m_i}(\dot{\delta}_i(t) - \dot{F}_i^*) \tag{28}$$

Introducing also Assumption 2, one has that

$$\frac{1}{m_i}\left|\dot{\delta}_i(t) - \dot{F}_i^*\right| \leq \frac{1}{m_i}\left(\hat{\Delta}_i + \hat{F}_i^*\right) \tag{29}$$

so that (26) enforces a sliding motion provided that

$$K_i > 2(\hat{\Delta}_i + \hat{F}_i^*) \tag{30}$$

Once attained $\sigma_i(t) = 0$, at time instant t_f, $\bar{v}_i(t) = v_i(t) \ \forall t \geq t_f$, which concludes the proof. ■

During the sliding mode, since $\bar{v}_i(t) = v_i(t)$, also $F_i^*(t) = 0 \ \forall t \geq t_f$ holds. Relying on the concept of equivalent control [21], one can then infer that

$$u_{ism_i}(t) = F_i^*(t) - \delta_i(t) = -\delta_i(t) \leq \Delta_i \tag{31}$$

holds in Filippov's sense and therefore in (20a) ρ must be chosen sufficiently larger than Δ_i to ensure feasibility also during the reaching phase.

Proposition 2: In *Case 2*, for the generic vehicle i and for a proper choice of K_i, if the corrective term is selected as

$$u_{ism_i,h} = -K_i sign\left(\sigma_{i,h} - \frac{\sigma_i^*}{2}\right) \tag{32}$$

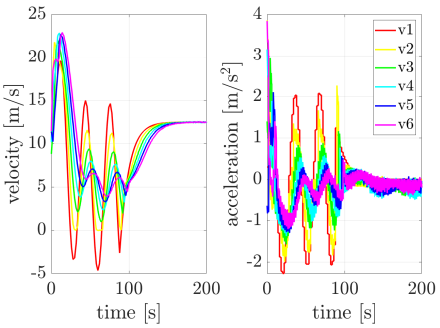

Fig. 3. *Case 1:* Velocity and acceleration profiles for the vehicles in the platoon, optimal control only.

the real velocity evolution tracks in finite time the nominal one, predicted relying on model (10).

Proof: Similar argumentations as the ones given above can be used also in this case, where

$$\begin{aligned}\ddot{\sigma}_i(t) = &\frac{1}{m_i\tau_i}\left(\bar{F}_{in_i}(t) - F_{in_i}(t) + \gamma_i(t) + \tau_i\left(\dot{\delta}_i(t) - \dot{F}_i^*\right)\right) \\ &+ \frac{1}{m_i\tau_i}u_{ism_i}(t)\end{aligned} \tag{33}$$

with $|\bar{F}_{in_i}(t) - F_{in_i}(t)|$ locally bounded by a certain known positive constant ΔF_{in_i}, since $\bar{F}_{in_i}(t)$ can never grow unbounded in practice. In order to enforce finite-time convergence, in this case

$$K_i > 2[(\Delta F_{in_i} + \Gamma_i + \tau_i(\hat{\Delta}_i + \hat{F}_i^*)] \tag{34}$$

must be ensured. ■

The κ term of Equation (20a) can be simply chosen such that $\kappa_i > K_i$. Notice how, in (34), the required control effort decreases with τ_i, i.e. with more "responsive" actuators, according with intuition.

IV. SIMULATION RESULTS

This section is devoted to present simulation results which validate the proposals of the present paper. In this scenario, the platoon is composed of 6 vehicles, considered here as having all the same nominal physical parameters (summarized in Table I) and settings of the control scheme reported in Table II. Random uncertainty is injected in the vehicle dynamics with the aim of simulating the previously mentioned mismatches between the models and the real systems, as well as possible external forces arising from actuation lags, unaccounted nonlinearities, etc. In particular, the following shifted low-frequency sinusoid, on which random uniform noise is superimposed, is used as uncertainty

$$\beta_{i_1} + \beta_{i_2} * \left[sin\left(\frac{1}{\beta_{i_3}}t + \beta_{i_4}\right) + r_i(t)\right] \tag{35}$$

both for $\delta(t)$ and $\gamma(t)$, where all the parameters β_i are constants randomly picked for each of the vehicles, while $r_i(t)$ is a uniform random variable. In particular, $\beta_{i_1} \in [-150;450]$, $\beta_{i_2} \in [0;450]$, $\beta_{i_3} \in [1;11]$, $\beta_{i_4} \in [0;5]$, $r_i(t) \in [0;0.25]$.

As one can see in Figure 3, the maneuver considered here is such that the leader initially follows a sinusoidal velocity,

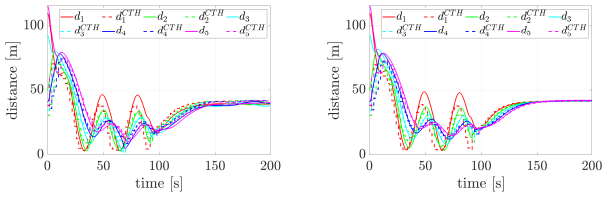

(a) Optimal control only. (b) ISM-robustified optimal control.

Fig. 4. *Case 1:* Distances between the vehicles. Solid lines refer to actual distances, dashed ones are the respective CTH references.

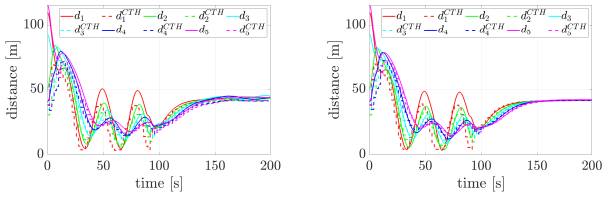

(a) Optimal control only. (b) ISM-robustified optimal control.

Fig. 5. *Case 2:* Distances between the vehicles. Solid lines refer to actual distances, dashed ones are the respective CTH references.

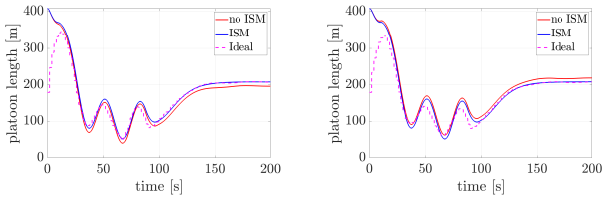

(a) *Case 1.* (b) *Case 2.*

Fig. 6. Total platoon length. The oscillations which appear in the second half of the maneuver, which are more and more present as the number of vehicles increase and represent lack of coherence, are cancelled by the ISM.

then starts to cruise at almost constant velocity for the rest of the time. The vehicles start at random initial positions and are able to merge into a platoon under the same control strategy presented in the paper (see Figures 4 and 5). In the former phase the velocity of the following vehicles is much smoother than that of the leader, and so is the acceleration, so that an overall decrease in the energy waste can reasonably be inferred as the consequence of the underlying behaviour of the MPC energy-aware distributed controllers. During the second phase, in which the platoon instead cruises, coherence is enforced by the introduction of the ISM correction term (Figure 6). The distances between vehicles are almost identical in both cases with the robust controller (compare Figures 4(b) and 5(b)), highlighting the insensitivity of the proposed scheme to uncertainty in spite of the fact that the MPC sampling time is as high as $2s$ and could be in principle increased even more.

V. CONCLUSIONS

The present paper proposes a robust multi-rate distributed MPC scheme for vehicles platoon control which relies on an ISM corrective term injection. Energy efficiency is addressed as desirable in acceleration/deceleration phases, where a clever prediction of the future situations is of crucial importance. During cruising coherence is kept in spite of uncertainty. Theoretical and simulation results show that the resulting system, if all of the vehicles involved are equipped with the presented control scheme, is robust against unknown perturbations in the velocity dynamics.

REFERENCES

[1] B. van Arem, C. J. G. van Driel, and R. Visser, "The impact of cooperative adaptive cruise control on traffic-flow characteristics," *IEEE Transactions on Intelligent Transportation Systems*, vol. 7, no. 4, pp. 429–436, Dec 2006.

[2] S. E. Li, Y. Zheng, K. Li, and J. Wang, "An overview of vehicular platoon control under the four-component framework," in *2015 IEEE Intelligent Vehicles Symposium (IV)*, June 2015, pp. 286–291.

[3] D. Jia, K. Lu, J. Wang, X. Zhang, and X. Shen, "A survey on platoon-based vehicular cyber-physical systems," *IEEE Communications Surveys Tutorials*, vol. 18, no. 1, pp. 263–284, Firstquarter 2016.

[4] A. Stotsky, C. C. Chien, and P. Ioannou, "Robust platoon-stable controller design for autonomous intelligent vehicles," in *Proceedings of 1994 33rd IEEE Conference on Decision and Control*, vol. 3, 1994.

[5] W. B. Dunbar and R. M. Murray, "Distributed receding horizon control for multi-vehicle formation stabilization," *Automatica*, vol. 42, no. 4, pp. 549 – 558, 2006.

[6] W. Dunbar and D. S. Caveney, "Distributed receding horizon control of vehicle platoons: Stability and string stability," *IEEE Transactions on Automatic Control*, vol. 57, pp. 620–633, 03 2012.

[7] J. Larson, K.-Y. Liang, and K. H. Johansson, "A distributed framework for coordinated heavy-duty vehicle platooning." *IEEE Trans. Intelligent Transportation Systems*, vol. 16, no. 1, pp. 419–429, 2015.

[8] Z. Ramezani, D. Gagliardi, and L. Del Re, "A risk-constrained and energy efficient stochastic approach for autonomous overtaking," in *Proceedings of the 2018 European Control Conference*, 2018.

[9] B. Bamieh, M. R. Jovanovic, P. Mitra, and S. Patterson, "Coherence in large-scale networks: Dimension-dependent limitations of local feedback," *IEEE Transactions on Automatic Control*, vol. 57, no. 9, pp. 2235–2249, Sept 2012.

[10] A. Ferrara, S. Sacone, and S. Siri, *Freeway Traffic Modelling and Control*. Springer International Publishing, 2018.

[11] F. Lin, M. Fardad, and M. R. Jovanović, "Optimal control of vehicular formations with nearest neighbor interactions," *IEEE Transactions on Automatic Control*, vol. 57, pp. 2203–2218, 2012.

[12] A. Ferrara and G. P. Incremona, "Design of an integral suboptimal second-order sliding mode controller for the robust motion control of robot manipulators," *IEEE Transactions on Control Systems Technology*, vol. 23, no. 6, pp. 2316–2325, 2015.

[13] G. Piacentini, P. Goatin, and A. Ferrara, "Traffic control via moving bottleneck of coordinated vehicles," *IFAC-PapersOnLine*, vol. 51, no. 9, pp. 13 – 18, 2018.

[14] A. Ferrara, Ed., *Sliding Mode Control of Vehicle Dynamics*. IET, London, 07 2017.

[15] M. Amodeo, A. Ferrara, R. Terzaghi, and C. Vecchio, "Wheel slip control via second-order sliding-mode generation," *IEEE Transactions on Intelligent Transportation Systems*, vol. 11, no. 1, pp. 122–131, 2010.

[16] A. Rupp, M. Steinberger, and M. Horn, "Sliding mode based platooning with non-zero initial spacing errors," *IEEE Control Systems Letters*, vol. 1, no. 2, pp. 274–279, 2017.

[17] E. Regolin, G. P. Incremona, and A. Ferrara, *Sliding mode control of vehicle dynamics*. IET, London, 2017, ch. Longitudinal Vehicle Dynamics Control via Sliding Modes Generation, pp. 33–76.

[18] L. Bertoni, J. Guanetti, M. Basso, M. Masoero, S. Cetinkunt, and F. Borrelli, "An adaptive cruise control for connected energy-saving electric vehicles," *IFAC-PapersOnLine*, vol. 50, no. 1, pp. 2359 – 2364, 2017.

[19] D. Swaroop and K. R. Rajagopal, "A review of constant time headway policy for automatic vehicle following," in *ITSC 2001. 2001 IEEE Intelligent Transportation Systems. Proceedings (Cat. No.01TH8585)*, Aug 2001, pp. 65–69.

[20] G. Bartolini, A. Ferrara, and E. Usai, "Chattering avoidance by second-order sliding mode control," *IEEE Transactions on Automatic Control*, vol. 43, no. 2, 02 1998.

[21] V. I. Utkin, *Sliding Modes in Control and Optimization*. Springer-Verlag, 1992.